

# MODIS-BASED OBSERVATION OF SEA-SURFACE CHLOROPHYLL-A CONCENTRATION OVER UPPER GULF OF THAILAND

Prasarn Intacharoen<sup>1,2</sup>, Songkot Dasananda<sup>1\*</sup> and Anukul Buranapratheprat<sup>2</sup>

*Received: September 10, 2017; Revised: February 05, 2018; Accepted: February 11, 2018*

## Abstract

This paper reports fruitful utilization of satellite-based MODIS optical data on sea-surface Chl-a concentration determination and mapping over Upper Gulf of Thailand (UGoT) region during 2010-2012 period. To fulfil this task, the optimal algorithm for extraction of the constituent through the applied MODIS reflectance data was identified first based on their effectiveness in determination of reference Chl-a data. The preferred Chl-a concentration maps were then generated through the identified algorithm along with their associated trophic state maps established regarding the modified OECD criteria. In the first step, the OC3M algorithm was selected (out of five initial candidates) as it provided the most satisfied output (with  $R^2$  of 0.60) and used to make Chl-a density maps for the area. These obtained maps indicated that the concerned critical areas which are potentially vulnerable to red-tide occurrence (i.e., those in eutrophic/hyper-eutrophic states with high amount of Chl-a mixture) were frequently assembled over shallow water close to shore and main surrounding river mouths in the north, especially that of the Tha Chin River. However, patterns and strength of their distribution over the area were remarkably dynamic all year round with relatively low activity evidenced in dry season and more pronounced situation seen in monsoon season. In this regard, notable drop in total amount of the critical areas during wet season of 2011 was attributed to the influence of mega-flooding over central Thailand at that time.

**Keywords:** Chlorophyll-a, MODIS, mega-flooding, trophic states, UGoT

---

<sup>1</sup> School of Remote sensing, Faculty of Science, Suranaree University of Technology, Nakorn Ratchasima, 30000, Thailand. E-mail: songkot@sut.ac.th

<sup>2</sup> Department of Aquatic Science, Faculty of Science, Burapha University, Chonburi, 20131, Thailand.

\* Corresponding author

## Introduction

In recent decades, critical degradation of marine ecosystem condition has been evidenced worldwide due mainly to massive discharge of waste from several land-based sources into coastal areas, especially those of the mega cities with dense population. One notable sign of this problem is an appearance of the eutrophication in coastal zone where water body is filled with an excess amount of nutrients. This process can induce dramatic growth of phytoplankton or algae colony over the area called the plankton/algae bloom (or red-tide phenomenon) which may lead to vital oxygen depletion and substantial amount of toxin in contaminated water. Typically, main driving factors of widespread eutrophication nowadays are population growth, excessive use of the fertilizer, and increase of industrialization (Khan and Aliansari, 2005; Helsinki Commission, 2009; Smith and Schindler, 2009; Ferreira *et al.*, 2011). High nutrient condition could fuel remarkably fast development of the red tide phenomenon with the cycle rate of appearing might be less than one week (Chuenniyom, Meksumpun, and Meksumpun, 2012).

To facilitate effective observation and monitoring of the red-tide incidence, several space-based optical sensors (e.g. SeaWiFS, MERIS, VIIRS, MODIS-Terra, MODIS-Aqua) were developed and applied for the identification and mapping of the plankton/algae bloom distribution worldwide (through prior knowledge of sea-surface Chl-a concentration of the area). Among which, the stated MODIS sensors are the most prominent nowadays due to their frequent revisit time at a specific area (4 times/day in the collaboration), relatively large observed area per scene, and notably high number of operating bands in both optical and thermal wavelengths (36 bands in total) (IOCCG, 2000; Ha *et al.*, 2014; Terauchi *et al.*, 2014).

For the Upper Gulf of Thailand (UGoT), occurrence of the red-tide situation was also more evidenced recently especially for areas close to the four major river mouths, i.e., the Bang Pakong, Chao Phraya, Mae Klong and

Tha Chin (Figure 1). This finding is often attributed to large amount of nutrient input from agriculture activities, mariculture industry, and household sewage. According to recent reports published by the Institute of Marine Science (2006), Department of Marine and Coastal Resources (2012), and recorded by author until of year 2015, there were more than 120 credible cases of the red-tide incidence observed over the UGoT area during 2004-2015 period. However, most red-tide data were normally taken from visual-sighting reports, scarce ship-based surveys, or near-shore fixed-point measuring stations, which are still not able to provide comprehensive and up-to-date information on occurrence frequency, precise location, or definite spatial extent of the seen event. This information is necessary for formulating better understanding on the origins, developing pattern, and associated impact of the event.

To overcome still shortcomings of traditional methods, implementation of the frequent satellite-based observation was introduced worldwide to attain more comprehensive data of the red-tide development over large area with encouraging results (Koponen *et al.*,

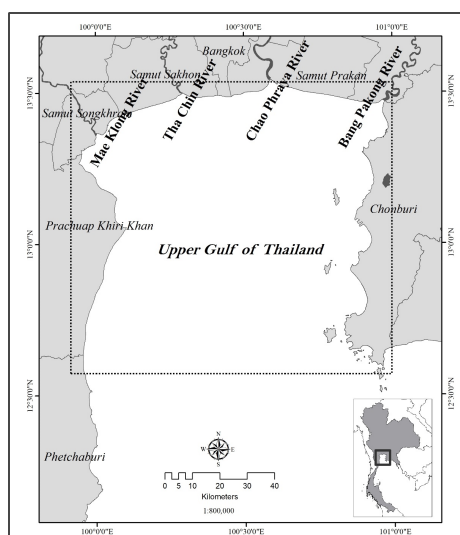


**Figure 1.** Map of the study area (UGoT)

2002; Buranapratheprat *et al.*, 2009; Marghany and Hashim, 2010). However, such works for the UGoT area were quite rare; e.g. Phoomwongpitak (2003) and Buranapratheprat *et al.* (2009), and none was carried out with MODIS data before.

This research aimed to identify optimal algorithm for effective observation and mapping of sea-surface Chl-a concentration over the UGoT from the referred MODIS reflectance data from which associated trophic-state maps were generated for water quality analysis purpose (using the classified red tide as prime indicator). The success of this work shall be greatly beneficial for the operation of rapid and up-to-date monitoring/mapping of the degraded water quality (due to

plankton/algal bloom scenario) over the UGoT territory in the near future.

## Materials and Method

### Data Collection and Preparation

Two principal sources of the input data used in this study are the observed MODIS reflectance data in 10 optical bands over the UGoT region downloaded from the MODIS website and the reference in-situ data of sea-surface radiance reflectance (from the PRR spectrometer) and Chl-a concentration data (extracted from samples of sea water collected during field surveys). Details of the main data preparation process are as follows:

**Table 1. Geographic coordinates of sampling sites in the UGoT**

| Station | Latitude (N) | Longitude (E) | Bottom Depth (m) |
|---------|--------------|---------------|------------------|
| 1       | 13 20.03     | 100 49.97     | 13.0             |
| 2       | 13 20.00     | 100 39.99     | 15.7             |
| 3       | 13 20.02     | 100 29.99     | 10.6             |
| 4       | 13 20.00     | 100 19.99     | 9.0              |
| 5       | 13 10.00     | 100 09.99     | 16.8             |
| 6       | 15 59.96     | 100 10.01     | 17.8             |
| 7       | 12 49.76     | 100 10.10     | 18.8             |
| 8       | 12 50.01     | 100 20.00     | 24.9             |
| 9       | 12 49.98     | 100 30.03     | 22.1             |
| 10      | 12 50.03     | 100 40.00     | 28.2             |
| 11      | 12 39.99     | 100 20.01     | 27.7             |
| 12      | 12 40.04     | 100 30.02     | 24.6             |
| 13      | 12 40.01     | 100 40.01     | 37.2             |
| 14      | 13 00.00     | 100 29.99     | 19.7             |
| 15      | 13 00.02     | 100 40.02     | 16.0             |
| 16      | 13 10.02     | 100 40.00     | 20.5             |
| 17      | 13 09.99     | 100 50.51     | 27.0             |

**Table 2. Five cruises surveys in UGoT**

| Cruise No. | Survey Periods      | Monsoon         | Seasonal |
|------------|---------------------|-----------------|----------|
| 1          | 09-11 October 2003  | Late southwest  | Wet      |
| 2          | 04-06 December 2003 | Early northeast | Dry      |
| 3          | 13-15 January 2004  | Late northeast  | Dry      |
| 4          | 12-15 May 2004      | Early Southwest | Dry      |
| 5          | 07-10 October 2004  | Late southwest  | Wet      |

Source: Matsumara *et al.*, 2006.

1) In-situ solar reflectance data in 6 spectral bands of the PRR instrument for 17 sampling sites over the UGoT region (as detailed in Figure 1 and Table 1). These data were assembled during the five main cruise surveys of the area during 2003-2004 in both wet and dry seasons as mentioned in Table 2 and later reported in Matsumura *et al.* (2006) (84 records in total). Technically, the PRR instrument can measure both downwelling and

upwelling of solar radiance at rather broad spectral range of 340-900 nm with 6 standard channels available centered at 412, 443, 490, 520, 565, 670 nm as illustrated in Table 3 (Horning *et al.*, 2010).

2) Corresponding sea-surface Chl-a concentration data at each specified sampling point determined through lab analysis of the collected water samples following standard

**Table 3. Spectral measurements of the PRR-2600 and 2610 instruments compared to those of the MODIS instruments at optical region**

| PRR-2600, 2610   |                | MODIS                      |                                    |                |
|------------------|----------------|----------------------------|------------------------------------|----------------|
| Band center (nm) | Bandwidth (nm) | Band no./ Band center (nm) | Wavebands products of Level 2 (nm) | Bandwidth (nm) |
| 412*             | 10             | 8 / 412                    | 412                                | 15             |
| 443*             | 10             | 9 / 443                    | 443                                | 10             |
|                  |                | 10 / 488                   | 469**                              | 10             |
|                  |                |                            | 488                                | 10             |
| 490*             | 10             |                            |                                    |                |
| 520*             | 10             | 11 / 531                   | 531                                | 10             |
|                  |                | 12 / 551                   | 547                                | 10             |
|                  |                |                            | 555**                              | 10             |
| 565*             | 10             |                            | 645**                              | 10             |
|                  |                | 13 / 667                   | 667                                | 10             |
| 670*             | 10             | 14 / 678                   | 678                                | 10             |
|                  |                | 15 / 748                   |                                    | 10             |
|                  |                | 16 / 869                   |                                    | 10             |

\* Spectral measurements of the PRR used in this study.

\*\* Generated from MODIS 250 m or 500 m data aggregated to 1 km.

Source: Horning *et al.* (2010).

**Table 4. Coefficient of determination ( $R^2$ ) of PRR reflectance and MODIS Level 2**

| PRR Wavelengths (nm) | MODIS Level 2 Wavelengths (nm) |      |      |      |      |      |      |      |      |      |
|----------------------|--------------------------------|------|------|------|------|------|------|------|------|------|
|                      | 412                            | 443  | 469  | 488  | 531  | 547  | 555  | 645  | 667  | 678  |
| 412                  | 0.67                           | 0.69 | 0.71 | 0.71 | -    | -    | -    | -    | -    | -    |
| 443                  | 0.64                           | 0.67 | 0.69 | 0.69 | -    | -    | -    | -    | -    | -    |
| 490                  | 0.62                           | 0.66 | 0.67 | 0.67 | -    | -    | -    | -    | -    | -    |
| 520                  | -                              | -    | -    | -    | 0.55 | 0.49 | 0.46 | -    | -    | -    |
| 565                  | -                              | -    | -    | -    | 0.53 | 0.50 | 0.49 | -    | -    | -    |
| 670                  | -                              | -    | -    | -    | -    | -    | -    | 0.28 | 0.28 | 0.28 |

guidelines given in Strickland and Parsons (1972).

3) Concurrent MODIS reflectance data level 2 (from NASA’s Terra/Aqua satellites) in 10 spectral bands (as described in Table 3) acquired from the public data archive over two main periods. The first one was for the 2003-2004 period in conjunction with the known operating dates of the referred cruise surveys reported in Table 1. This dataset was applied for analysing suitable replacement of the PRR data needed in the preferred retrieval algorithm by the corresponding MODIS one. The second one was for the 2010-2012 period accumulated on daily basis to serve as input for the quantifying and mapping of the Chl-a concentration distribution and its classified water quality condition at that time. Ten

MODIS spectral bands were considered including the blue-band group (at 412, 443, 469 and 488 nm), green-band group (at 531, 547 and 555 nm) and red-band group (at 645, 667 and 678 nm) as described in Table 3.

**Optimal Retrieval Algorithm Identification and Application**

To identify optimal retrieval algorithm for Chl-a concentration extraction from prior knowledge of the related solar reflectance data gathered from the PRR instrument, five established algorithms were considered as potential candidates for this task as listed in Table 5. In this process, sampling data of Chl-a concentration from 5 field surveys (84 records in total) were separated into two broad groups at random; one for the

**Table 5. Modified empirical algorithms for Chlorophyll-a estimation based on in situ and PRR dataset**

| No. | Algorithms name                            | Algorithms structure  | PRR modified structure   | Validation     |      |        | Remark   |
|-----|--|---|--|----------------|------|--------|--|
|     |  |   |  | R <sup>2</sup> | RMSE | MAPE   |  |
| 1   | OC3M (O’Reilly et al., 2000).              | $C_{chl-a} = 10^{(a_0+a_1R+a_2R^2+a_3R^3+a_4R^4)}$<br>$R = \log_{10} \left[ \max \left( \frac{R_{rs}(443)}{R_{rs}(550)}, \frac{R_{rs}(490)}{R_{rs}(550)} \right) \right]$ | $C_{chl-a} = 10^{(0.0513-1.5884R-5.5887R^2-5.4592R^3+16.977R^4)}$<br>$R = \log_{10} \left[ \max \left( \frac{R_{rs}(443)}{R_{rs}(565)}, \frac{R_{rs}(490)}{R_{rs}(565)} \right) \right]$ | 0.60           | 3.25 | 68.23  | Replaced Rrs 550 by 565  |
| 2   | Red to Green band ratio (Le et al., 2012). | $\ln(Chla) = a \ln(x) + b$<br>$x = \frac{[R_{rs}(678)]}{[R_{rs}(531) + R_{rs}(547)]}$   | $\ln(Chla) = 1.2475 \ln(x) + 2.7387$<br>$x = \frac{[R_{rs}(670)]}{[R_{rs}(520) + R_{rs}(565)]}$  | 0.27           | 3.54 | 78.43  | Excluded Rrs 667, replaced 678 by 670, 531 by 520 and 547 by 565 |
| 3   | rGBr (Ha, Koike, and Nhuan, 2014).         | $C_{chl-a} = C_1 \frac{R_{rs}(551)}{R_{rs}(443)} + C_2$   | $C_{chl-a} = 0.6828 \left( \frac{R_{rs}(565)}{R_{rs}(443)} \right) + 0.1842$   | 0.22           | 3.00 | 212.95 | Rrs 551 replaced by 565  |
| 4   | Applied SeaWiFs to MODIS (Tassan, 1994).   | $C_{chl-a} = \frac{[R_{rs}(443)]}{[R_{rs}(555)]} [R_{rs}(412)/R_{rs}(490)]^{-0.5}$  | $C_{chl-a} = 5.1419e^{-1.87x}$<br>$X = \frac{[R_{rs}(443)]}{[R_{rs}(565)]} \left[ \frac{[R_{rs}(412)]}{[R_{rs}(490)]} \right]^{-0.5}$  | 0.50           | 3.07 | 67.90  | Replaced Rrs 555 by 565  |
| 5   | Chula (Matsumura et al., 2006).            | $C_{chl-a} = 181.4 \exp^{-(-4.74R)}$<br>$R = R_{rs}(520)/R_{rs}(565)$   | $C_{chl-a} = 30.511 \exp^{-(-3.647R)}$<br>$R = R_{rs}(520)/R_{rs}(565)$  | 0.55           | 3.21 | 68.64  | -  |

**Table 6 The performance of Chlorophyll-a algorithms based on PRR-based prediction**

| Order | Algorithms name          | R <sup>2</sup> | RMSE | MAPE   |
|-------|--------------------------|----------------|------|--------|
| 1     | OC3M                     | 0.60           | 3.23 | 68.23  |
| 2     | Chula                    | 0.55           | 3.21 | 68.64  |
| 3     | Applied SeaWiFs to MODIS | 0.50           | 3.07 | 67.90  |
| 4     | Red to Green band ratio  | 0.27           | 3.35 | 78.43  |
| 5     | rGBr                     | 0.22           | 3.00 | 212.95 |

construction of best-fit structure for each evaluated candidate (70%) and the other one for the assessment of their yielded prediction efficiency (30%). Effectiveness of each considered candidate on predicting amount of Chl-a density from known solar reflectance input was determined from three following parameters: coefficient of determination ( $R^2$ ), root mean square error (RMSE) and mean absolute percentage error (MAPE), from which an optimal method was then identified. And the PRR-based parameters appeared in the optimal algorithm were subsequently replaced by their relevant MODIS-based counterparts which exhibit highest correlation level between them (as reported in Table 4).

The found MODIS-based optimal algorithm was then operated to produce density maps of the sea-surface Chl-a over UGoT area from years 2010 to 2012 on

daily (to monthly) basis as shown in Figure 2 in which 240 MODIS imageries were implemented. These derived maps were then analyzed to acquire knowledge on variation patterns of Chl-a concentration over the whole UGoT region during that stated period as well as their implications on red-tide occurrence and water quality degradation. Among these, notable impact of the 2011 mega flooding over central Thailand on the observed water quality of the UGoT coastal zone (from MODIS image data) was also investigated. For water quality evaluation, the original Chl-a density maps were used to produce their trophic-state map counterparts according to the applied OECD criteria (described in Table 8). From the formulated trophic-state maps, the potential red-tide incidences were then identified for areas located in the classified eutrophic and hyper-eutrophic zones (i.e., the low quality

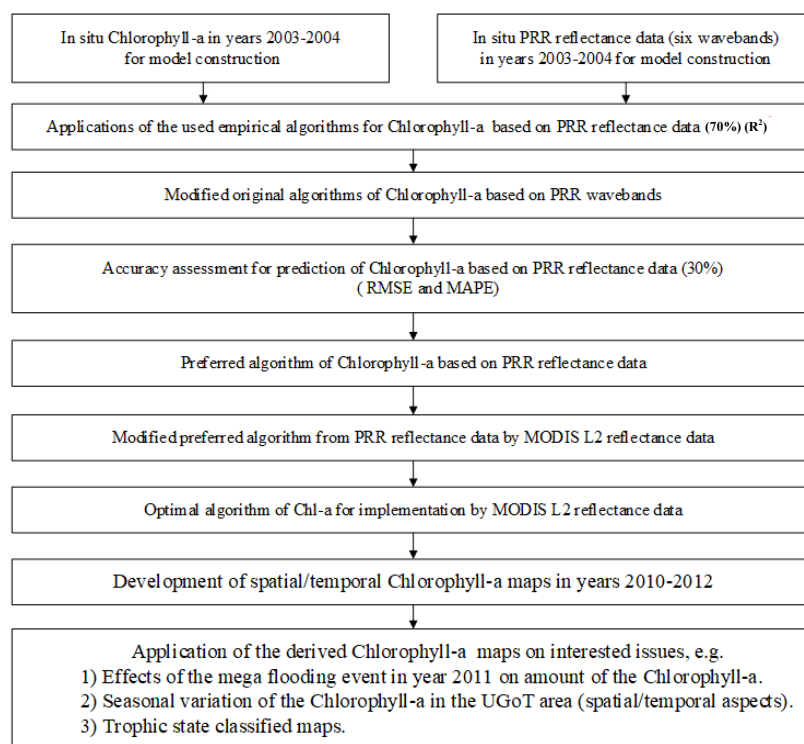


**Figure 2. Workflow of the empirical algorithm method and Chlorophyll-a variation in UGoT base on MODIS data**

region). This red-tide map outcome is valuable for the investigation of water crisis hotspots along with their causes and effects over the area.

## Results and Discussion

### Optimal Algorithm for Chl-a Concentration Extraction

Five candidates for the Chl-a retrieval operation were empirically modified to suit available spectral bands of the applied PRR instrument (as listed in Table 3) in which original wavelength-specific input data were replaced by the PRR band data with closest wavelength location (as illustrated in Table 5). For example, three wavelength-specific input data (at 443, 490, 550 nm) of the used OC3M algorithm were replaced by the closest band data of the PRR instrument (at 443, 490, 565 nm respectively). Apart from this, appropriate values of the coefficients and constants appeared in each assessed algorithm were also derived empirically from the found best-fit solution (to the reference Chl-a output

dataset) as demonstrated in Figure 4 for the OC3M case. Capability of these modified algorithms (as shown in Table 5) in predicting accurate Chl-a concentration output (from the PRR radiance input) were then assessed based on results of three standard indicators mentioned earlier, i.e.,  $R^2$ , RMSE and MAPE. Results of the analysis are as reported in Table 6, from which the modified OC3M algorithm was considered an optimal candidate for this task due to its highest  $R^2$  (of 0.60) and comparative low RMSE and MAPE output regarding those of other candidates. The PRR-based parameters seen in the OC3M algorithm were then replaced by their specific MODIS-based representatives based on their exhibited correlation strength reported in Table 4 (i.e., 490 nm by 488 nm and 565 nm by 531 nm). From this modification, the MODIS-based OC3M model was achieved and put to use in the quantification and mapping of Chl-a density over the UGoT study area on daily-to-monthly basis through which the Chl-a map (on 4<sup>th</sup> December 2003) was given as an example in Figure 5 with maximum value of

**Table 7. The optimal algorithm for Chlorophyll-a extraction based on MODIS data (OC3M)**

| Algorithm | PRR modified structure  | MODIS implement   | Remark                                 |
|-----------|---|---|--|
| OC3M      | $C_{chl a} = 10^{\left( \frac{0.0513 - 1.5884R - 5.5887R^2 - 5.4592R^3}{+16.977R^4} \right)}$ $R = \log_{10} \left[ \max \left( \frac{R_{rs}(443)}{R_{rs}(565)}, \frac{R_{rs}(490)}{R_{rs}(565)} \right) \right]$ | $C_{chl a} = 10^{\left( \frac{0.0513 - 1.5884R - 5.5887R^2 - 5.4592R^3}{+16.977R^4} \right)}$ $R = \log_{10} \left[ \max \left( \frac{R_{rs}(443)}{R_{rs}(531)}, \frac{R_{rs}(488)}{R_{rs}(531)} \right) \right]$ | Replaced Rrs 490 by 488 and 565 by 531 |

**Table 8. Modified of OECD Fixed Boundary System for the UGoT performance**

| Trophic state      | Mean Chlorophyll-a (µg/l) |
|--------------------|---------------------------|
| Ultra-oligotrophic | ≤ 1.0                     |
| Oligotrophic       | ≤ 2.5                     |
| Mesotrophic        | 2.5 – 8.0                 |
| Eutrophic          | 8.0 – 25.0                |
| Hyper-eutrophic    | ≥ 25.0                    |

Source: OECD, 1982

37.693 mg/m<sup>3</sup> and minimum one of 0.037 mg/m<sup>3</sup> recorded.

### Chl-a Observation and Mapping Between 2010-2012

The modified OC3M was then used to generate Chl-a concentration maps for the UGoT area during 2010-2012 period from daily MODIS spectral radiance input data (at spatial resolution of 1 km) from which the developed daily maps of Chl-a density were later integrated to produce corresponding monthly mean maps for each studied year as displayed in Figures 6-8, respectively. These map outputs provide information on variation pattern of Chl-a concentration over the UGoT in both space and time aspects. In conclusion, for 2010, high concentration of Chl-a in average was evidenced in rainy season from June to September, with maximum value of about 91.28 mg/m<sup>3</sup> in September, while the lowest concentration appeared in March at 4.68 mg/m<sup>3</sup> (Table 9 and Figure 9). High density of the Chl-a substance were often seen close to shore and main attached river mouths, especially those of the Mae Klong and Tha Chin Rivers.

However, in 2011, top values of the derived concentration data occurred in dry season towards early wet season (from March to July) as expressed in Table 9 with highest value of 104.08 mg/m<sup>3</sup> in June. After that, maximum concentration of Chl-a over the

UGoT area were started to decline sharply towards the end of year with lowest data witnessed in December (at 20.608 mg/m<sup>3</sup>). The prominent drop in Chl-a intensity from August to December this year coincided well with the period of large influx of freshwater releasing into the UGoT through the attached river mouths from the 2011 mega flooding occurring over central Thailand (Figure 3). This excessive load of inland water could lead to more nutrient volume in nearby sea water with less concentration outcome due to the strong dilution effect. Note that, due to the lack of valid MODIS data in September 2011, Chl-a map was also not available. This makes the analysis about impact of the 2011 mega flooding on Chl-a strength and distribution over the UGoT area still partly inconclusive.

In 2012, more fluctuation was observed with peak values of Chl-a density appeared in April (44.431 mg/m<sup>3</sup>), June (46.134 mg/m<sup>3</sup>) and October (49.723 mg/m<sup>3</sup>) while the hotspot areas were often evidenced close to shore and around the river mouths as expected. However, peak values of the derived Chl-a density were not as high as those gained in 2010 and 2011. In general, variation patterns of maximum and mean values of the extracted Chl-a density in 2011 and 2012 were somewhat resemble but those of the 2010 were distinctively different from the others.

In this work, 2010 was regarded as a normal year, and the achieved results

**Table 9. Standard statistics of Chlorophyll-a concentration during 2010-2012 period**

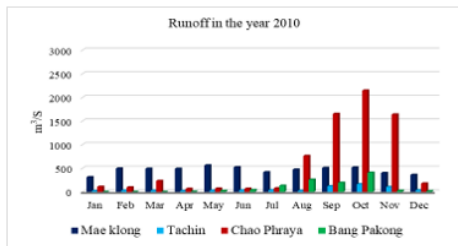
| Month/<br>Year | Maximum<br>(mg/m <sup>3</sup> ) |        |       | Minimum<br>(mg/m <sup>3</sup> ) |      |       | Mean<br>(mg/m <sup>3</sup> ) |      |      | Std Dev.<br>(mg/m <sup>3</sup> ) |      |      |
|----------------|---------------------------------|--------|-------|---------------------------------|------|-------|------------------------------|------|------|----------------------------------|------|------|
|                | 2010                            | 2011   | 2012  | 2010                            | 2011 | 2012  | 2010                         | 2011 | 2012 | 2010                             | 2011 | 2012 |
| January        | 12.72                           | 21.72  | 20.88 | 0.21                            | 0.31 | 0.120 | 1.56                         | 2.04 | 1.99 | 1.35                             | 2.47 | 2.47 |
| February       | 8.91                            | 33.21  | 18.66 | 0.24                            | 0.17 | 0.107 | 1.23                         | 1.58 | 1.57 | 0.77                             | 2.11 | 1.77 |
| March          | 4.68                            | 87.87  | 13.97 | 0.29                            | 0.13 | 0.139 | 1.21                         | 1.95 | 1.29 | 0.49                             | 4.05 | 1.00 |
| April          | 18.53                           | 65.41  | 44.43 | 0.24                            | 0.10 | 0.091 | 1.99                         | 2.03 | 1.47 | 2.06                             | 3.76 | 3.05 |
| May            | 21.96                           | 93.77  | 23.34 | 0.27                            | 0.09 | 0.237 | 2.52                         | 2.23 | 1.41 | 2.96                             | 4.36 | 1.29 |
| June           | 45.34                           | 104.08 | 46.13 | 0.44                            | 0.09 | 0.272 | 4.22                         | 2.27 | 2.14 | 5.26                             | 5.02 | 4.05 |
| July           | 88.03                           | 49.13  | 34.98 | 0.31                            | 0.10 | 0.287 | 5.13                         | 2.80 | 2.06 | 7.68                             | 4.14 | 3.08 |
| August         | 46.82                           | 33.48  | 18.91 | 0.37                            | 0.42 | 0.229 | 3.33                         | 2.12 | 1.68 | 4.39                             | 2.10 | 1.67 |
| September      | 91.28                           | NA     | 17.42 | 0.31                            | NA   | 0.229 | 5.03                         | NA   | 1.91 | 8.59                             | NA   | 1.97 |
| October        | 26.32                           | 25.62  | 49.72 | 0.42                            | 0.12 | 0.128 | 2.88                         | 2.32 | 2.71 | 2.65                             | 1.92 | 2.79 |
| November       | 22.63                           | 26.43  | 44.96 | 0.40                            | 0.17 | 0.031 | 2.43                         | 3.21 | 2.90 | 2.87                             | 3.04 | 3.99 |
| December       | 26.70                           | 20.61  | 29.64 | 0.35                            | 0.31 | 0.043 | 2.23                         | 2.09 | 2.08 | 2.81                             | 2.16 | 2.52 |



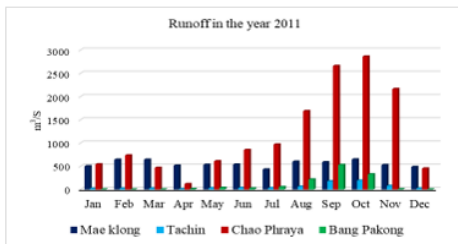
(as displayed in Figure 9 and Table 9) indicate that mean and maximum output of derived Chl-a density values tended to be lowest during dry season (January-April). The pigment intensity then rose steadily towards wet season (May to September), with notable drop in August, before coming to end around September from which gradual fall was noticed throughout winter. This finding was supported by relevant work of Boonkwan (2013) which found the highest diversity index in August and the lowest in March. Thaipichitburapa (2013) also reported higher amount of Chl-a concentration in wet season

than in dry season at the Tha Chin River mouth and loaded nutrients in water were high in almost entire year. In addition, Wattayakorn and Jaiboon (2014) found that the observed photosynthesis activity was larger than decomposition plus bottom release during wet season while those activities were similar in dry season which indicated Chl-a concentration in wet season should be higher than in dry season for the UGoT area.

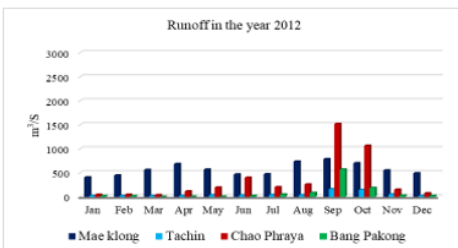
Years 2011 and 2012 were regarded as flood-affected years in this work, therefore, variation trends of the Chl-a concentration over the area (maximum and mean) were



(a) Four main river discharges in the year 2010.



(b) Four main river discharges in the year 2011.



(c) Four main river discharges in the year 2012.

Source: Royal irrigation department, 2015.

Figure 3. Four main river discharges from years 2010 to 2012

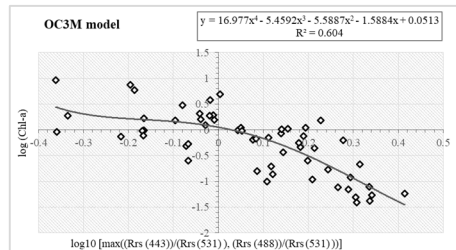


Figure 4. PRR-based OC3M algorithm performance for Chlorophyll-a prediction

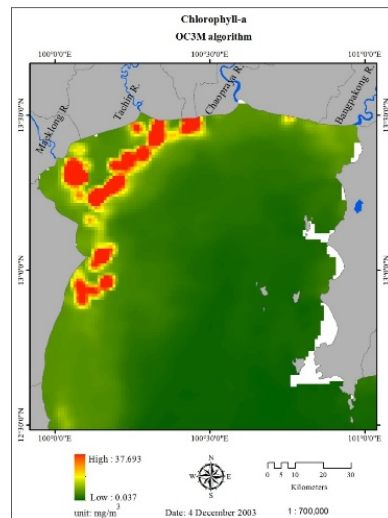


Figure 5. MODIS-based Chlorophyll-a concentration map derived by the OC3M algorithm on 4<sup>th</sup> December 2003

expected to have different characteristics compared to those of 2010 (considered a normal year). These differences were strongly evidenced during time of mega-flood appearance (August-December, 2011) when key observed Chl-a data (maximum and mean) dropped significantly compared to those of 2010 due to huge dilution impact from large excessive amount of flood water coming to the UGoT near-shore area. However, these differences were less obvious when flood's effect gradually declined in 2012.

### Trophic States Over UGoT Area from Years 2010 to 2012

Knowledge of top-layer Chl-a concentration distribution in the sea area is useful for the assessment of trophic states over the area based on the classification criteria proposed by the OECD in 1982. In general, trophic state indicates amount of the nutrient loading in the water body for which amount of Chl-a concentration is commonly used as its standard objective classifier. For this work, five trophic states were systematically mapped based on value of mean observed Chl-a density suggested by the OECD (in Table 8), which

are (from low to high nutrient loading level); (1) ultra-oligotrophic (UT), (2) oligotrophic (OT), (3) mesotrophic (MT), (4) eutrophic (ET), (5) hyper-eutrophic (HT). Regarding this criterion, monthly trophic level maps for the whole UGoT area during 2010-2012 period were constructed from the associated monthly Chl-a density maps (in Figures 6-8) and the obtained results are demonstrated in Figures 10-12, respectively.

From this output, ultra-oligotrophic and oligotrophic states, i.e. the healthy states with low amount of growth nutrient loading and high amount of dissolved oxygen, were found predominant in deep-water zone further away from land and the main river's mouths. On the contrary, eutrophic and hyper-eutrophic states, i.e. the unhealthy states with relatively high amount of nutrient loading, were mostly appeared on areas close to shore and to main river mouths as expected. However, strength level and distributing pattern of these incidences might vary from year to year under influence of several factors. For examples, in 2010, the occurrences of the concerned eutrophic/hyper-eutrophic (ET/HT) incidences were relatively low during dry months

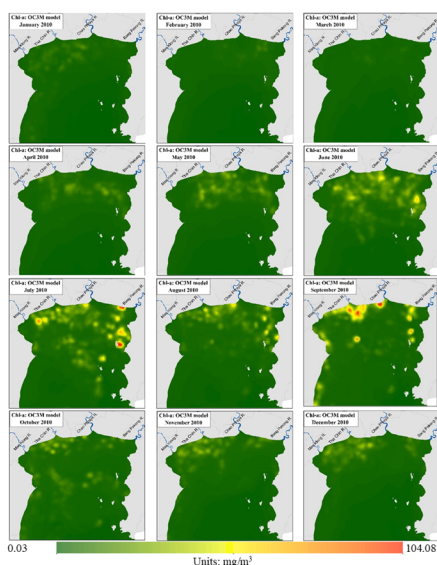


Figure 6. Spatial distribution of monthly Chlorophyll-a concentration in 2010

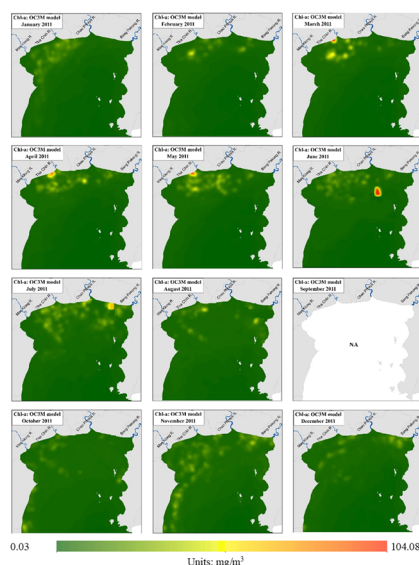


Figure 7. Spatial distribution of monthly Chlorophyll-a concentration in 2011

(January-April) but their distribution and apparent strength were notably amplified throughout the wet season (June-September), especially for areas in the vicinity the Chao

Phraya, Tha Chin and Bang Pakong river mouths (where most loaded nutrients are supposed to reside). In 2011, more widespread of the concerned critical states (ET/HT) was

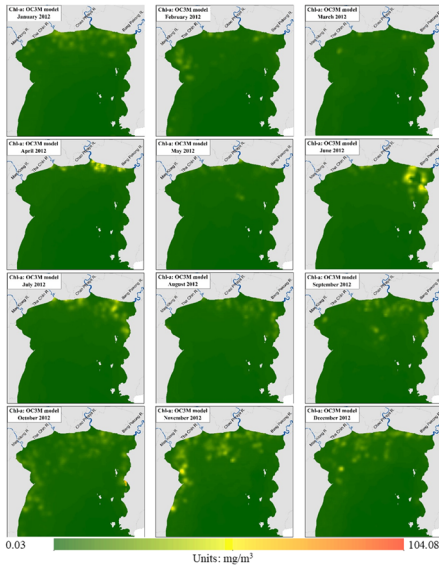
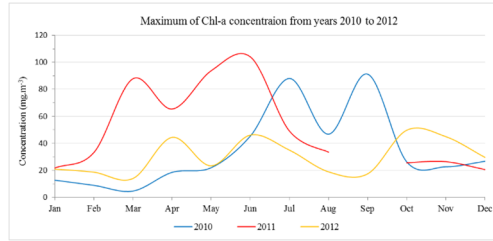
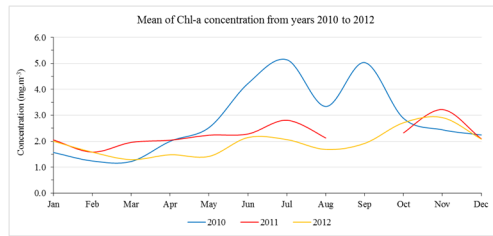


Figure 8. Spatial distribution of monthly Chlorophyll-a concentration in 2012



(a) Maximum concentration of Chl-a



Mean concentration of Chl-a

Figure 9. Maximum/mean Chlorophyll-a concentration data in 2010 - 2012 (OC3M model)

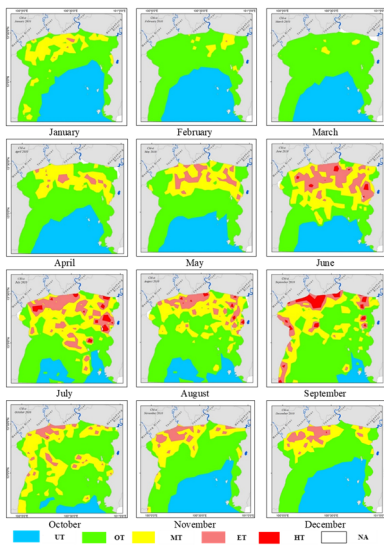


Figure 10. Trophic state maps of Chlorophyll-a based on OC3M model in 2010

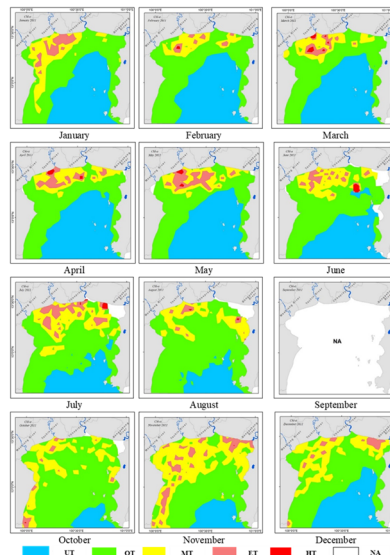


Figure 11. Trophic state maps of Chlorophyll-a based on OC3M model in 2011

evidenced in dry season, especially around the Tha Chin river mouth. However, remarkable drop of critical conditions during 2011 wet season (June-August) was observed compared to those of 2010 (the normal year). This was supposed to be due to influence of the mega-flooding event over central Thailand as described earlier.

In 2012, severity of the critical situation in general was not as widespread as in 2011 during dry months but it was getting more extreme over the wet season and the winter period towards the end of the year (June-

December). Here, two most critical months were noted including prominent expansion of the HT state in June and the ET in November. During dry season, the critical hotspots were found located mostly along the NE coast, close to the Bang Pakong River’s mouth, but in November, those areas were more widespread covering many parts of coastal zones, especially along the NW coast close to Mae Klong River’s mouth.

### Conclusions

This paper reports fruitful applications of the identified optimal MODIS-based retrieval algorithm (OC3M) on the quantification and mapping of sea-surface Chl-a concentration and its associated trophic state over the UGoT region during the 2010-2012 period which had never been done before. Results obtained therein indicated that low amount of the Chl-a mixture was usually identified further away from shore over the deep water zone. On the contrary, the critical areas, i.e. ones with notably high Chl-a density in eutrophic (ET) and hyper-eutrophic (HT) states, were typically located close to upper shore in the vicinity of the surrounding river mouths as expected, especially that of the Tha Chin River.

However, during 2010-2012, distributing pattern and apparent intensity of the critical events (ET/HT) were rather dynamic all year round. For examples, in 2010, defined critical scenarios were relatively low in dry season (January-April) but they appeared to rise rapidly towards monsoon season (with peaks seen in July and September) before having remarkable drop in strength towards the end of the year. In 2011, more widespread critical clusters were visible in dry season (often linked to mouth of the Tha Chin River) but situation was not getting much worse in monsoon season as in 2010. This was attributed to large excessive influx of fresh water from massive floods over central Thailand that happened during that time. In 2012, critical scenes were not spectacular all year round except some noticeable surge seen

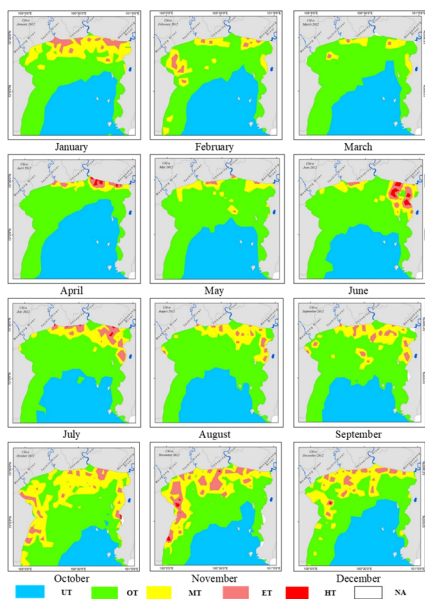


Figure 12. Trophic state maps of Chl-a based on OC3M model in 2012

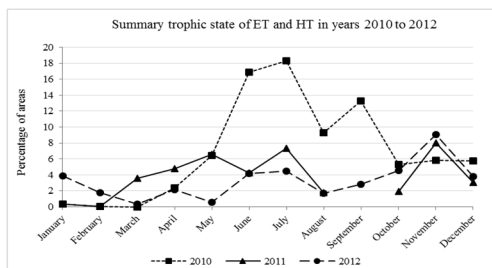


Figure 13. Area proportion of the ET/HT trophic states from 2010 to 2012

in June (associated to the Bang Pakong River's mouth) and November (along the western coastal zone).

Comprehensive knowledge gained from these aforementioned works could improve initial understanding on Chl-a distribution and its impact on water quality (e.g. on red-tide formation) over the UGoT region in the near future. They also provide guidelines for developing more effective local algorithm for the extraction of Chl-a and other important water constituents, e.g. suspended solid or CDOM, from the appropriate ocean-based satellite dataset (apart from MODIS) like those of the SeaWiFS, MERIS, OCTS, OLI/Landsat 8 and VIIRS sensors for Thailand. In addition, routine space-based monitoring for the early red-tide occurrences over the UGoT (like one demonstrated in this work) and hotspot location analysis were recommended for warning and damage mitigation purposes from the incidences.

## Acknowledgements

Contribution of the cruises data of the Upper Gulf of Thailand for this research by Prof. Dr. Satsuki Matsumura is gratefully acknowledged.

## References

- Bhatrasataponkul, T. (2004). Development of ocean colour algorithms for the Upper Gulf of Thailand. Master of Science dissertation, Department of Marine Science, Faculty of Science, Chulalongkorn University, Thailand.
- Biospherical Instruments Inc. (2002). User's manual profiling reflectance radiometer system (PRR-2600). 5340 Riley Street San Diego, CA 92110-2621. Version 004961UC.DOC.
- Boonkwan, S. (2013). Seasonal variations of phytoplankton and primary production in the inner gulf of Thailand. Master of science dissertation in Aquatic science, Burapha University, Thailand.
- Buranapratheprat, A., Niemann, K. O., Matsumura, S., and Yanagi, T. (2009). MERIS imageries to investigate surface chlorophyll in the upper Gulf of Thailand. *Coastal Marine Science.*, 33(1): 22-28.
- Chuenniyom, W., Meksumpun, C., and Meksumpun, S. (2012). Impacts of nutrients and related environmental factors on distribution and size structure of *Noctiluca scintillans* populations of the eutrophic Tha Chin Estuary, Thailand. *Water Sci. Tech.*, 65:11.
- Department of Marine and Coastal Resources. (2012). Red tide phenomenon. Available from: <http://www.mkh.in.th/index.php/2010-03-22-18-05-34/2010-03-26-07-59-54>. Accessed date: June 29, 2012.
- Ferreira, J.G., Andersen, J.H., Borja, A., Bricker, S.B., Camp, J., da Silva, M.C., Garcés, E., Heiskanen, A.-S., Humborg, C., Ignatiades, L., Lancelot, C., Menesguen, A., Tett, P., Hoepffner, N., and Claussen, U. (2011). Overview of eutrophication indicators to assess environmental status within the European Marine Strategy Framework Directive. *Estuar. Coast. Shelf S.*, 93(2):117-131.
- Ha, N.T.T., Koike, K., and Nhuan, M.T. (2014). Improved accuracy of chlorophyll-a concentration estimates from MODIS imagery using a two-band ratio algorithm and geostatistics: As applied to the monitoring of eutrophication processes over Tien Yen Bay (Northern Vietnam). *Remote Sens.*, 6:421-442.
- Helsinki Commission. (2009). Eutrophication in the Baltic Sea. Helsinki Commission. [On-line]. Available: <http://www.helcom.fi/stc/files/Publications/Proceedings/bsep115A.pdf>
- Horning, N., Robinson, J.A., Sterling, E.J., Turner, W., and Spector, S. (2010). Remote sensing for ecology and conservation: a handbook of techniques. United States: Oxford University Press Inc., NY.
- Institute of Marine Science. (2006). Marine environmental monitoring program and protection management of red tide in the coastal water of Chonburi Province. Burapha University, Thailand.
- IOCCG. (2000). Remote sensing of ocean colour in coastal, and other optically-complex, waters. In Stuart, V. (Ed.), Reports of the International Ocean-Colour Coordinating Group. Dartmouth, Canada. 3:140.
- Keith, D.J., Yoder, J.A., and Freeman, S.A. (2002). Spatial and temporal distribution of coloured dissolved organic matter (CDOM) in Narragansett Bay, Rhode Island: implications for phytoplankton in coastal waters. *Estuarine Coastal and Shelf Science.*, 55(5):705-717.
- Khan, F.A. and Aliansari, A. (2005). Eutrophication: an ecological vision. *Bot. Rev.*, 71(4):449-482.
- Koponen, S., Pulliainen, J., Kallio, K., and Hallikainen, M. (2002). Lake water quality classification with airborne hyperspectral spectrometer and simulated MERIS data. *Remote Sens. Environ.*, 79:51-59.
- Marghany, M. and Hashim, M. (2010). MODIS satellite data for modelling chlorophyll-a concentrations in Malaysian coastal waters. *Int. J. Phy. Sci.*, 5(10):7.
- Matsumura, S., Siripon, A., and Lirdwitayaprasit, T. (2006). Underwater optical environment in the Upper Gulf of Thailand. *Coastal Marine Sci.*, 30(1):36-43.
- OECD. (1982). Eutrophication of waters: monitoring, assessment and control. Organization for economic and co-operative development, Paris, France. Quoted in Stednick, J.D. and Hall, E.B. (2003). Applicability of trophic status indicators to

- colorado plains reservoirs. Completion Report No. 195. Colorado Water Resources Research Institute. Colorado State University, USA.
- Phoomwongpitak, W. (2003). Meteorological factors associated with chlorophyll-a concentration in the gulf of Thailand as studied by remote sensing technique. Master of environmental science disertation. Chulalongkorn University, Thailand.
- Smith, V.H. and Schindler, D.W. (2009). Eutrophication science: where do we go from here?. *Trends in Ecol. Evolu.*, 24(4):201-207.
- Terauchi, G., Tsujimoto, R., Ishizaka, J., and Nakata, H. (2014). Preliminary assessment of eutrophication by remotely sensed chlorophyll-a in Toyama Bay, the Sea of Japan. *J. Oceanogr.*, 70(2):175-184.
- Thaipichitburapa, P. (2013). Pesticide dynamic model for aquatic ecosystem of Tha-Chin River, Thailand. Doctoral thesis, Kasetsart University. Thailand.
- Wattayakorn, G. and Jaiboon, P. (2014). An assessment of biogeochemical cycles of nutrients in the inner gulf of Thailand. *Euro. Chem. Bull.*, 3(1):50-54.